Design of an electronic charged particle spectrometer to measure $\langle \rho \mathscr{R} \rangle$ on inertial fusion experiments

D. G. Hicks, C. K. Li, R. D. Petrasso, and F. H. Séguin
Plasma Fusion Center, Massachusetts Institute of Technology, Cambridge, Massachusetts

B. E. Burke
Lincoln Laboratory, Massachusetts Institute of Technology, Lexington, Massachusetts

J. P. Knauer, S. Cremer, and R. L. Kremens
Laboratory for Laser Energetics, University of Rochester, Rochester, New York 14623

M. D. Cable and T. W. Phillips
Lawrence Livermore National Laboratory, Livermore, California 94550

(Presented on 14 May 1996)

The design and fabrication of a new diagnostic that measures the energy spectra of charged particles from targets on the Omega Upgrade are actively underway. Using seven 512×512 charge coupled devices (CCDs) and a 7.5 kG permanent magnet, this instrument will uniquely determine particle identities and measure particle energies from 1 MeV up to the maximum charged particle energies of interest for ρR measurements (10.6 MeV knock-on tritons, 12.5 MeV knock-on deuterons and 30.8 MeV tertiary protons). The resolution of the diagnostic will be better than 5%. We have tested the response of SITe back-illuminated CCDs to 1.2–13.6 MeV protons from our Cockcroft–Walton accelerator and to alpha particles from an Am^{241} source, and the results agree extremely well with predictions. With its high density picture elements, each CCD has 10^5 single-hit detectors. In the case of a low DT yield of 10^9 neutrons, about 100 knock-on charged particles will be detected when the spectrometer aperture is 60 cm from the implosion. Measurements of ρR up to 150 mg/cm^2 can be obtained from knock-on D and T spectra, and values up to 300 mg/cm^2 can be determined from secondary proton spectra. The sensitivity of the CCDs to 14 and 2.5 MeV neutrons has been experimentally determined using our Cockcroft–Walton accelerator source and indicates that by incorporating neutron shielding, the signal to neutron noise ratio at a yield of 10^{11} will be better than 100:1. In the development phases of this program, we plan to utilize CR-39 track detectors concurrently with the CCDs. [S0034-6748(97)57301-1]

I. INTRODUCTION

The progress of inertial fusion experiments towards higher ρR's and ignition makes nuclear fusion product detectors crucial for diagnosing conditions within the target. The charged particle spectrum from 1 to 30.8 MeV produced by an imploding inertial fusion DT target provides information about fuel and pusher ρR as well as implosion symmetry (if diagnostics at two or more different positions are used simultaneously). The main reactions generating such charged particles are the elastic scattering of D and T fuel ions by 14.1 MeV neutrons (producing knock-on deuteron and triton energies up to 12.5 and 10.6 MeV, respectively) and the burn up of nascent 0.82 MeV ^{3}He ions, born of DD reactions, producing secondary protons from 12.5 up to 17.4 MeV. Both the yield and spectral degradation of these MeV charged particles can be used to determine fuel and pusher ρR's.[1–10] The knock-on method has an upper limit of $\rho R \sim 150$ mg/cm^2 (above which the knock-ons are ranged out) while the energy degradation of secondary protons may be used to determine ρR's up to 300 mg/cm^2 (above which secondary protons are ranged out for a 1 keV plasma). At higher ρR's the spectrum of tertiary protons up to 30.8 MeV must be used to diagnose ρR using charged particles.[11]

The fusion burn within imploding targets typically occurs within a time interval of order 1 ns; thus, in order to obtain a reasonable charged particle spectrum, the energy and identity of hundreds of charged particles must be gathered within this period.

To date, only CR-39 track detectors and nuclear emulsion detectors have been used to detect inertial confinement fusion (ICF) charged particles. While the simplicity and low cost of these detectors ensures that they will be used in conjunction with this diagnostic, they involve laborious, off-line analysis techniques.

We present the design for an electronic charged particle spectrometer that utilizes the high pixel density of charge coupled device (CCD) technology to discriminate individual particles spatially and thus avoid pulse pile-up. We have verified experimentally the viability of using CCD technology to resolve spectrally charged particles of several MeV. The concept for this design was first outlined in Ref. 12.

II. THE INSTRUMENT

A. The concept

The challenge of determining the energy spectrum of protons, deuterons, and tritons from an ICF target is that for every particle there are two quantities to be measured: the energy and the mass. To determine these independent unknowns, two measurements must be made. In the past, much of the difficulty with track studies of charged particles from

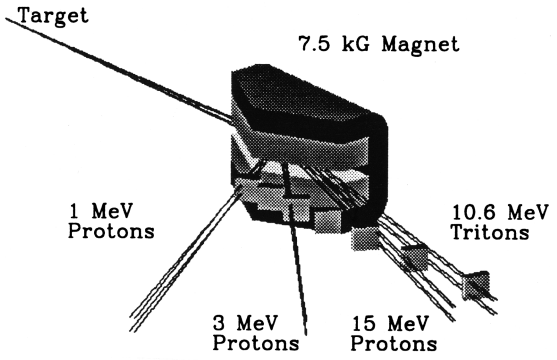

FIG. 1. The 7.5 kG pentagonal permanent magnet; 7 CCDs; particle trajectories for 1 MeV protons, 3 MeV protons, 15 MeV protons, and 10.6 MeV tritons. The magnet and yoke structure is 28 cm long, 17 cm wide (to the apex), and 20 cm high. Particle path lengths within the magnet are in the range of 20–25 cm.

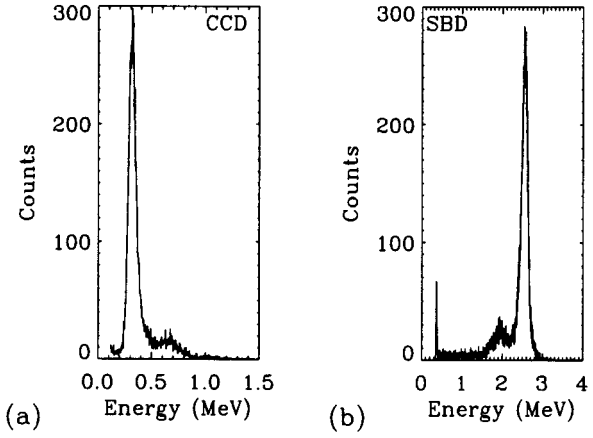

FIG. 2. The 2.6 MeV proton spectrum as measured simultaneously by a back-illuminated CCD (a) and a surface barrier diode (b).

DT targets has stemmed from the limited ability to determine whether an individual track of a particular diameter was due to a proton, deuteron, or triton; difficult techniques involving precise thicknesses of track material and ranging filters were required to eliminate all but one type of particle from the signal. For example, since the track diameter is a function of the particle velocity, 9 MeV tritons, 6 MeV deuterons, and 3 MeV protons would all produce the same signal (CCDs face an equivalent degeneracy problem).

To overcome this degeneracy, we incorporate a 7.5 kG dipole magnet to disperse the particles before they are detected, enabling the position of the particle event in the detector plane to be used as a second measurement. The 9 MeV tritons, 6 MeV deuterons and 3 MeV protons, though they have the same velocity (a function of mass/energy), have different gyroradii in a magnetic field (a function of mass $\times$energy) and thus arrive at different positions in the detector plane. Every event is thus characterized not only by its ''size,'' i.e., track diameter for etch detectors and pixel brightness for CCDs, but also by its position—two measurements to measure two unknowns. In addition, the magnet not only performs the simple task of breaking the mass degeneracy, but also provides energy information (in the fashion of a typical magnetic spectrometer). The layout of our proposed magnet and CCD system is shown in Fig. 1.

B. The magnet

The design of the magnet was driven by the need to view a particle spectrum from 1 MeV protons (particles with the smallest gyroradius) up to 10.6 MeV tritons (particles with the largest gyroradius) and to maximize the particle signal. The entire diagnostic must fit into a cone whose apex is at the target and whose sides are constrained by the laser beam positions. With these considerations, the 7.5 kG Nd–Fe–B dipole magnet shown in Fig. 1 is being constructed by Dexter Corporation.[13] The pentagonal shape was necessary to allow the magnet to get close to the target without violating the limits of the cone. The magnet has a 2 cm gap with better than 2% field uniformity in its central region. Use of 1.5-cm-thick shunts to smooth edge fields reduces fringing fields to 50 G 7 cm from the magnet.

C. The CCDs

CCDs are extremely sensitive detectors of radiation and can easily detect individual charged particles in the MeV range, which deposit 10–100 times as much energy as x rays of a few keV. Unlike x rays, charged particles deposit their energy along their entire path through silicon, allowing them to be detected with 100% quantum efficiency. However, since the sensitive depth of a typical back-illuminated CCD is usually no more than 10–15 μm, and since light ions in the MeV range have a range of tens to hundreds of microns in silicon, only a fraction of the incident particle energy is recorded by the device. Nevertheless, through the use of well-known stopping formulas, such as the Bethe–Bloch formula, and a known value for the sensitive depth, the energy recorded by the CCD is a direct measure of the incident particle energy for a given particle type.

We have performed extensive tests using protons and α's on back-illuminated CCDs[14] [from Scientific Imaging Technologies, Inc. (SITE)[15]] and front-illuminated CCDs[16] (from Lincoln Laboratory). A typical CCD proton spectrum for the back-illuminated device is shown in Fig. 2 and compared to the surface barrier diode (SBD) spectrum for the same particle energy. It is clear that these CCDs have excellent energy response to charged particles and show no obvious mechanisms for charge loss, even though events are often spread over more than one pixel.[17] By bombarding these CCDs with a range of known proton energies from our Cockcroft–Walton accelerator and a range of known α energies from an Am^{241} source, we have mapped out the energy response curves of such devices and plotted them in Fig. 3. The data closely match the energy response predicted from stopping power curves assuming a sensitive depth of 14 μm as specified by the manufacturer.

The CCD energy response curves are plotted in units of Energy$\times A/Z^2$ (proportional to the square of the local gyroradius) since this is the parameter that determines the degree of dispersion of the particle in the magnetic field. The positioning of a particular CCD in the dispersed particle beam exiting the magnet determines the energy window that it will see as shown in Fig. 3. Within this restricted energy window,

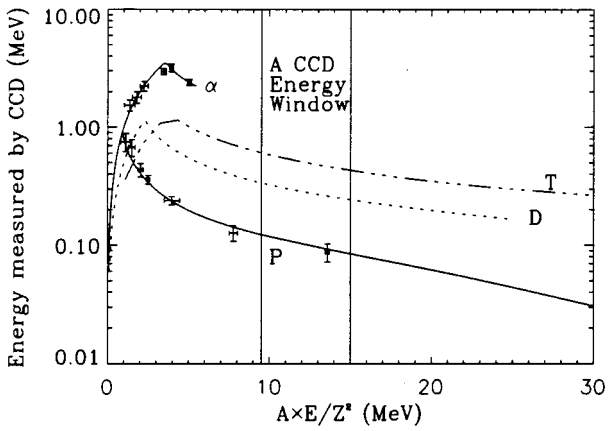

FIG. 3. The energy response curves for particles of different gyroradii incident normally on a SITe back-illuminated CCD with a sensitive depth of 14 μm. Within a particular energy window defined by the position of the CCD in the dispersed beam, particles of different mass generate very different CCD responses, enabling unique particle discrimination.

it is possible to uniquely attribute every particle event to a proton, deuteron, or triton at a specific energy, breaking the degeneracies that existed without the magnet (where the detector would see all particles at all energies).

D. The integrated system

A diagram of the integrated magnet and CCD system is shown in Fig. 4. The support module mounted to the vacuum chamber wall allows the magnet entrance slit to be placed as close as 60 cm from the target. Much of structure volume and the region outside the structure, between the magnet and the target, is filled with lead-impregnated, borated polyethylene (Pb–B–PE) to thermalize and capture a substantial fraction of the copious direct and scattered neutrons and gammas generated by the target. A beam dump is incorporated to minimize the number of scattered neutrons and γ's from the direct line of sight. For high yield shots, the entire magnet and CCD system can be retracted, while for low yield shots, the magnet entrance slit is adjustable up to 2 cm wide and 1 cm high. The slit is covered by a light tight, 25 μm beryllium

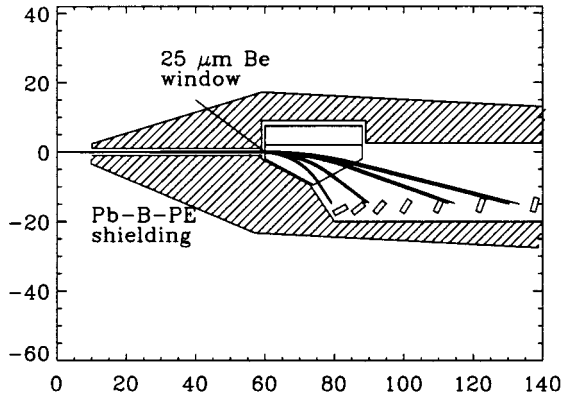

FIG. 4. In order to minimize direct and scattered neutron and gamma noise, large amounts of Pb–B–PE shielding will be incorporated (dimensions in cm).

window to prevent laser and other light sources in the visible and near visible range from flooding the detectors. In addition, this window (and other insertable windows) will allow this entire diagnostic system to maintain a vacuum separate from that of the target chamber, enabling easy access into the diagnostic area when maintenance is required. Seven 512 $\times$512 CCDs are placed in the exit plane as shown to cover the energy range from 1 MeV protons up to 10.6 MeV tritons. Each CCD is cooled to ~ -20 °C using thermoelectric coolers. The CCDs and their electronics are custom configured to allow the arrays to be placed as close together as possible, minimizing dead space. Data is transferred via fiber optic cables to minimize electronic pick-up.

III. PREDICTED PERFORMANCE

A. Energy resolution

The energy resolution of this device is determined both by the CCDs and the magnet. Our conservative estimate puts the total CCD resolution at better than 5%. For a slit width of 5 mm, the magnet resolution varies from 1% at the low energies to 9% at the high energies. For this and smaller slit widths, the magnet provides resolution comparable to that of the CCD.

B. Operating yield

For lower-yield experiments, the diagnostic will operate at 60 cm from the target with a 1-cm-high by 2-cm-wide entrance slit, giving a solid angle of 4.4×10^{-5} steradians. At a yield of 10^9 DT neutrons and a ρR of 10 mg/cm^2, $\sim$100 knock-ons will be detected. When the neutron yield is 10^{13}, a 1-cm-high by 1-mm-wide magnet entrance slit placed at the vacuum wall—$\sim$160 cm from the target—will result in detection of $\sim10^4$ knock-ons when $\rho R=10$ mg/cm^2. This diagnostic can thus span four orders of magnitude in DT yield.

C. Signal-to-noise

The main sources of noise in our system will be from the 14 MeV neutrons and their associated gammas—both direct and scattered. Due to the complex nature of the interactions of neutrons with the surrounding target chamber, it is extremely difficult to precisely predict the noise sensitivity of the CCD to this type of radiation environment. We plan to measure this sensitivity inside a Ten Inch Manipulator (TIM) on the Omega Upgrade. In order to obtain an estimate of these noise levels however, we have exposed our CCDs to 14 MeV neutrons from our Cockcroft–Walton accelerator and determined an ''effective'' neutron sensitivity of 2×10^{-3}. A simple calculation of the number of direct neutron interactions with the sensitive region of the CCD yields a sensitivity lower by a factor of 20, and we believe that this discrepancy is caused by the associated gamma interactions. However, since most of these interactions occur in the lower energy region, below our lowest charged particle signal levels, most of them may be rejected.

Furthermore, the magnet provides an additional means of noise rejection: Since each CCD is restricted to viewing a

narrow particle energy window by virtue of its position in the dispersed particle beam, any noise events that occur outside this designated energy window can be discarded. Thus a calculation of the instrument signal-to-noise ratio using our neutron data must take into account the spectral quality of the neutron interactions, and not just the absolute sensitivity. In addition, MCNP calculations and our experimental measurements have indicated that 60 cm of Pb–B–PE shielding attenuates the neutron flux by more than a factor of 100.

With these considerations, we present a sample signal-to-noise calculation for a DT yield of 10^{11} and $\rho R = 10$ mg/cm^2 with the 5 mm$\times$1 cm magnet slit at 60 cm from the target. For the 512$\times$512 CCD in the high-energy part of the dispersed beam, 350 tritons (from 6.2–10.6 MeV) and 200 deuteron knock-ons (from 9.3–12.5 MeV) will be detected. The number of neutron and associated gamma events in these ranges that we predict on the basis of our CCD neutron measurements, lead to signal-to-noise ratios of 160:1 for the tritons and 400:1 for the deuterons.

D. CCD damage

While testing the response of 512$\times$512 SITe CCDs to protons, alphas, and neutrons, we have seen an increase in the dark current level of individual pixels with irradiation levels of $\sim 10^9$/cm^2, probably due to single-hit damage. On a cooled device that is read out rapidly, the effects of this increased dark current are negligible for our purposes. The levels of irradiation on the Omega Upgrade are expected to be much lower than those to which we have already exposed our device.

E. CR-39 track detectors

As mentioned earlier, we intend to utilize CR-39 track detectors throughout the development of this diagnostic in order to establish that our CCDs are behaving correctly. Preliminary data will be obtained by placing track detectors and one or two CCDs in the detector plane of the magnet. Since the energy resolution of CR-39 is poor (compared to CCDs), the track-based spectrometer will derive its energy resolution from the magnet. The presence of the magnet removes many of the limitations placed on CR-39 detectors in previous studies of knock-on, charged particle spectra.

IV. CONCLUSIONS

The design for a charged particle spectrometer using seven 512$\times$512 CCDs and a 7.5 kG permanent magnet has been described. With this design, D, T, and H knock-ons and secondary and tertiary protons may be measured from 1 MeV up to their maximum energies. With about 10^5 picture elements over an individual CCD, each element virtually being a single-hit detector, this spectrometer will function over four orders of magnitude of DT fusion yield. The energy resolution of the overall system is better than 5%, reaching 1% at low energies. The partially overdetermined nature of this diagnostic allows many spurious noise effects, such as those from neutrons and associated gammas, to be discarded from the signal. By incorporating large amounts of shielding, the signal-to-noise ratio for this diagnostic is determined to be better than 100:1.

ACKNOWLEDGMENTS

This work was supported in part by the Laboratory for Laser Energetics (University of Rochester), in part by the Department of Energy, and in part by Lawrence Livermore National Laboratory.

[1] S. Skupsky and S. Kacenjar, J. Appl. Phys. **52**, 2608 (1981).
[2] S. Kacenjar, S. Skupsky, A. Entenberg, L. Goldman, and M. Richardson, Phys. Rev. Lett. **49**, 463 (1982).
[3] S. Kacenjar, L. M. Goldman, A. Entenberg, and S. Skupsky, J. Appl. Phys. **56**, 2027 (1984).
[4] T. E. Blue, J. W. Blue, J. S. Durham, D. B. Harris, A. S. Hnesh, and J. J. Reyes, J. Appl. Phys. **54**, 615 (1983).
[5] H. Azechi, N. Miyanaga, R. O. Stapf, K. Itoga, H. Nakaishi, M. Yamanaka, H. Shiraga, R. Tsuji, S. Ido, K. Nishihara, Y. Izawa, T. Yamanaka, and C. Yamanaka, Appl. Phys. Lett. **49**, 555 (1986).
[6] F. J. Marshall, S. A. Letzring, C. P. Verdon, S. Skupsky, R. L. Keck, J. P. Knauer, R. L. Kremens, D. K. Bradley, T. Kessler, J. Delettrez, H. Kim, J. M. Soures, and R. L. McCrory, Phys. Rev. A **40**, 2547 (1989).
[7] H. Azechi, M. D. Cable, and R. O. Stapf, Laser and Particle Beams **9**, 119 (1991).
[8] J. Nakaishi, N. Miyanaga, H. Azechi, M. Yamanaka, T. Yamanaka, M. Takagi, T. Jitsuno, and S. Nakai, Appl. Phys. Lett. **54**, 1308 (1989).
[9] Y. Kitagawa, K. A. Tanaka, M. Nakai, T. Yamanaka, K. Nishihara, H. Azechi, N. Miyanaga, T. Norimatsu, T. Kanabe, C. Chen, A. Richard, M. Sato, H. Furukawa, and S. Nakai, Phys. Rev. Lett. **75**, 3130 (1995).
[10] C. K. Li and R. D. Petrasso, Phys. Rev. Lett. **70**, 3059 (1993).
[11] R. D. Petrasso, C. K. Li, M. D. Cable, S. M. Pollaine, S. W. Haan, T. P. Bernat, J. D. Kilkenny, S. Cremer, J. P. Knauer, C. P. Verdon, and R. L. Kremens, Phys. Rev. Lett. **77**, 2718 (1996).
[12] D. G. Hicks, C. K. Li, R. D. Petrasso, K. W. Wenzel, and J. P. Knauer, Plasma Fusion Center Report No. PFC/RR-94-11 (unpublished).
[13] Dexter Corporation, Magnetic Materials Division (PERMAG) 48460 Kato Rd., Fremont, CA 94538.
[14] C. K. Li, D. G. Hicks, R. D. Petrasso, F. H. Séguin, M. C. Cable, T. Phillips, J. P. Knauer, S. Cremer, and R. L. Kremens, Rev. Sci. Instrum., these proceedings.
[15] Scientific Imaging Technologies, Inc., P.O. Box 569, Beaverton, OR 97075.
[16] B. E. Burke, R. D. Petrasso, C. K. Li, and T. C. Hotaling, Rev. Sci. Insktrum., these proceedings.
[17] F. H. Seguin, D. G. Hicks, C. K. Li, R. D. Petrasso, M. C. Cable, and J. P. Knauer, Rev. Sci. Instrum., these proceedings.